ISIJ International, Vol. 48 (2008), No. 2, pp. 154–160

Effect of Height and Position of Dams on Inclusion Removal in a Six Strand Tundish

Pradeep K. JHA,[1] P. Srinivasa RAO[2] and Anupam DEWAN[2]

1) Department of Mechanical & Industrial Engineering, Indian Institute of Technology, Roorkee, Roorkee–247667, India.
2) Department of Mechanical Engineering, Indian Institute of Technology, Guwahati, Guwahati–781039, India.

(*Received on August 21, 2007; accepted on November 27, 2007*)

The Reynolds-averaged Navier–Stokes equations have been numerically solved to obtain a steady, three-dimensional velocity field inside the six-strand billet caster tundish using the standard k–ε model of turbulence. These steady flow fields so obtained are then used to predict the removal of inclusions from molten steel by solving the inclusion transport equation with the help of a commercial CFD software Fluent 6.1.22. The effects of height and position of dams in the tundish and size of the inclusion particles on percentage inclusion removal were studied. To simulate the chaotic effect of the turbulent eddies on the particle paths; a discrete random walk model was applied during inclusion trajectory calculations. The computational model was first validated with the results reported in the literature a good match was found between the two. It was found that with the increase in the height of the dams, the inclusion removal tendency increased whereas the shifting of the dams towards the outlets decreases the inclusion removal. An increase in the inclusion removal was found with an increase in the inclusion particle size.

KEY WORDS: continuous casting tundish; inclusion removal; particle size; dams.

1. Introduction

Tundish is an intermediate reservoir, placed between the ladle and the mold in a continuous casting unit. It, being the last stage for the steel before reaching into the mold, plays an important role in removing any inclusion particle resulting from sources like de-oxidation and re-oxidation products, slag entrapment, exogenous inclusions and many chemical reactions.[1] Being lighter than the molten steel, the inclusions present in the steel may be removed either by floating to the top slag (mostly for larger inclusion particles) or by sticking to the tundish walls[2–5] (for smaller particles). Use of flow modifiers is reported to promote the flow in the tundish towards the top surface which helps the inclusions float and get trapped by the slag layer at the top surface.[6–11]

Several studies[3,4,12–19] have been carried out for investigating flow and inclusion behavior in tundishes. Tacke and Ludwig[3] and Kaufmann *et al.*[4] studied inclusion flotation based on the scalar diffusion through an isothermal 3-D turbulent flow field. Tozawa *et al.*[12] and Sinha *et al.*[13] have developed models to simulate inclusion flotation in a tundish which account for the inclusion coalescence. It has further been investigated by many researchers[13–17] that if adequate time were provided, there would be better opportunity for the larger particles to float out at the surface of the tundish. Miki and Thomas[18] simulated the inclusion removal in a single strand tundish with flow modifiers using three different models. Zhang *et al.*[19] studied the three-dimensional fluid flow in continuous casting tundishes with and without flow control devices with the use of random walk model to incorporate the effect of turbulent fluctuations on the particle motion.

Most of these studies discuss the inclusion removal mechanism in single strand slab caster tundish. Study of multi-strand billet caster tundish with regard to its inclusion separation tendency from each one of the outlets has not been carried out. The presence of more than one outlet makes the study of multi-strand tundish more important as the inclusions passing through each outlet will determine the quality of the billets coming through each strand. In the present study, steady flow in a six-strand delta shape billet caster tundish is simulated with a 3-D finite-volume computational model using the standard k–ε turbulence model. The commercial software Fluent 6.1.22[20] is used for performing the flow simulations. Inclusion trajectories are calculated by integrating each local velocity, considering its drag and buoyancy forces. A "random walk" model[18] is used to incorporate the effect of turbulent fluctuations on the particle motion. The effect of height and position of dams placed before the outlets on the fluid flow and particle motion (for different particle size) in the tundish has been investigated.

2. Physical Description of the Problem

The geometry of the multi strand tundish used in present study is shown in **Fig. 1**(a). Half of the tundish is shown because of the symmetry about the inlet plane. The depth of the tundish is 572 mm with the size of the inlet as

© 2008 ISIJ

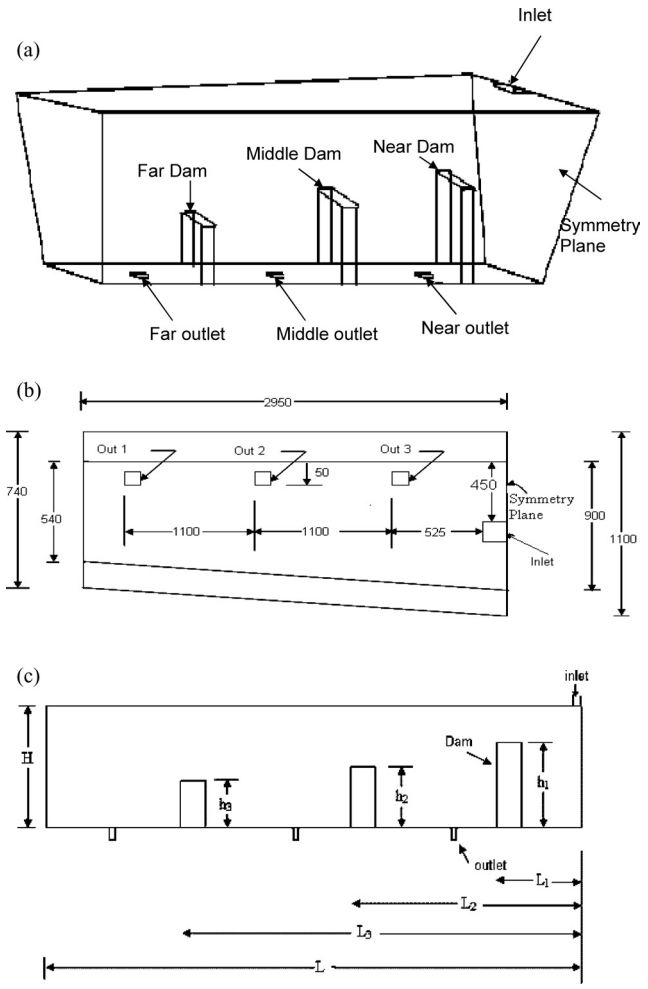


Fig. 1. (a) Geometry of the six-strand billet caster tundish, (b) plan view of the tundish, (c) notations about geometrical parameters.

25 mm×50 mm and all other dimensions are shown in a plan view in Fig. 1(b). The outlets are placed 50 mm away from the wall. Figure. 1(c) shows the two parameters, the height of the dams (Near Dam, Middle Dam and Far dam) and the distance of the dams from the inlet. Three different values of dam heights (Height 1, Height 2 and Height 3) and three different values of the distance of dams from the inlet representing different positions (Position-a, Position-b and Position-c) has been used (constituting all together 9 different cases) to study the effect of dam height and their position on inclusion floatation behaviour of the tundish. **Table 1** shows the different values of dam heights and their positions as described in Fig 1(c). Dimensionless heights of the dams, h_x* is defined as the ratio of height of the dam to the height of tundish (H). Dimensionless distance of the dams from the inlet (L_x*) is defined as the ratio of distance of dams from the inlet to the half tundish length (L). In defining the dimensionless parameter, x has value of 1, 2 and 3 where the three numbers refer to near dam (N.D.), middle dam (M.D.) and far dam (F.D.) respectively. Each case is named as AB where A is an integer from 1 to 3 representing three different height combinations of the dam (in increasing order) and B indicates the different dam positions *i.e.* position-a, b and c respectively (the distance from the inlet being in increasing order). The values of H and L are 572 mm and 2 950 mm respectively. Details of the values of the dimensionless parameters for different cases have been presented in **Table 2**.

Table 1. Description of different cases (with different combinations of dam heights and their positions).

Height of Dams								
Height-1			Height-2			Height-3		
N.D. (h_1)	M.D. (h_2)	F.D. (h_3)	N.D. (h_1)	M.D. (h_2)	F.D. (h_3)	N.D. (h_1)	M.D. (h_2)	F.D. (h_3)
200	150	100	250	200	150	300	250	200
Distance of Dams from inlet								
Position-a			Position-b			Position-c		
N.D. (L_1)	M.D. (L_2)	F.D. (L_3)	N.D. (L_1)	M.D. (L_2)	F.D. (L_3)	N.D. (L_1)	M.D. (L_2)	F.D. (L_3)
250	950	1950	300	1100	2150	350	1250	2350

3. Mathematical Formulation

3.1. Governing Equations for Fluid Flow and Inclusion Motion[2,19,21)]

Continuity:

$$\frac{\partial u_i}{\partial x_i} = 0$$

Momentum:

$$\frac{\partial}{\partial x_i}\rho u_i u_j = -\frac{\partial P}{\partial x_i} + \frac{\partial}{\partial x_i}\left(\mu_{\text{eff}}\left(\frac{\partial u_i}{\partial x_j} + \frac{\partial u_j}{\partial x_i}\right)\right) \quad ....(1)$$

$$\text{Where } \mu_{\text{eff}} = \mu_0 + \mu_t = \mu_0 + \rho C_\mu \frac{k^2}{\varepsilon} \quad .....(2)$$

Turbulent kinetic energy k:

$$U_j \frac{\partial k}{\partial x_j} = D_k + P - \varepsilon \quad .....(3)$$

Rate of dissipation of k:

$$U_j \frac{\partial \varepsilon}{\partial x_j} = D_\varepsilon + C_1 P \frac{\varepsilon}{k} - C_2 \frac{\varepsilon^2}{k} \quad .....(4)$$

where,

$$\overline{u_i u_j} = \frac{2}{3} k\delta_{ij} - \nu_t\left(\frac{\partial U_i}{\partial x_j} + \frac{\partial U_j}{\partial x_i}\right)$$

$$\nu_t = 0.09\frac{k^2}{\varepsilon}, \quad \mu_{\text{eff}} = \rho\nu_t + \mu,$$

$$D_\phi = \frac{\partial}{\partial x_j}\left[\left(\mu + \frac{\mu_t}{\sigma_\phi}\right)\frac{\partial \phi}{\partial x_j}\right]$$

$$P = -\overline{u_i u_j}\frac{\partial U_i}{\partial x_j}$$

The set of partial differential Eqs. (1) to (4) were first

© 2008 ISIJ

Table 2. Description of different cases with regard to different combinations of dimensionless heights and dimensionless distances of the dams.

Case	Dimensionless height of dams, h_x^* ($h_x^* = h_x / H$, x=1,2,3)			Dimensionless distance of dams, L_x^* ($L_x^* = L_x / L$, x=1,2,3)		
	N.D. (h_1^*)	M.D. (h_2^*)	F.D. (h_3^*)	N.D.(L_1^*)	M.D. (L_2^*)	F.D. (L_3^*)
1a	0.35	0.26	0.17	0.09	0.32	0.66
2a	0.44	0.35	0.26	0.09	0.32	0.66
3a	0.52	0.44	0.35	0.09	0.32	0.66
1b	0.35	0.26	0.17	0.10	0.37	0.73
2b	0.44	0.35	0.26	0.10	0.37	0.73
3b	0.52	0.44	0.35	0.10	0.37	0.73
1c	0.35	0.26	0.17	0.12	0.42	0.80
2c	0.44	0.35	0.26	0.12	0.42	0.80
3c	0.52	0.44	0.35	0.12	0.42	0.80

N.D.: Near Dam M.D.: Middle Dam F.D.: Far Dam

H Tundish bath height (572 mm)

L Half length of Tundish (2950 mm)

Table 3. Details of number of inclusions coming out and percentage removal from different outlet for different cases (particle size=30 μm).

Case	No of Inclusion Particles Passing Out (Total no of inclusions = 1080)				Percentage removal of inclusions from			
	N.O.	M.O.	F.O.	Overall	N.O.	M.O.	F.O.	Overall
Bare	260	180	107	547	75.92	83.33	90.09	49.35
1a	186	142	87	415	82.45	86.60	91.79	60.84
2a	163	131	74	368	84.62	87.64	93.01	65.28
3a	130	98	82	310	87.73	90.75	92.26	70.75
1b	186	143	88	417	82.45	86.50	91.69	60.66
2b	165	131	74	370	84.43	87.64	93.01	65.09
3b	141	102	95	338	86.69	90.37	91.03	68.11
1c	192	145	87	424	81.88	86.32	91.79	60.00
2c	166	135	71	372	84.33	87.26	93.30	64.90
3c	158	121	78	357	85.07	88.58	92.64	66.32

N.O. : Near outlet M.O. : Middle outlet F.O. : Far outlet

solved along with appropriate boundary conditions (mentioned in Sec. 3.2) numerically using finite volume approach. Inclusion trajectories were calculated using a Lagrangian particle tracking method, which solves a transport equation for each inclusion as it travels through the previously calculated steady state flow field. The mean local inclusion velocity components, u_p needed to obtain the particle path, were obtained from the following force balance, which includes drag and buoyancy forces relative to the steel.

$$\frac{du_p}{dt} = F_D(u-u_p) + \frac{g_x(\rho_p-\rho)}{\rho_p} + F_x \quad \text{.....(5)}$$

$F_D(U-U_p)$ is the drag force per unit mass of the particle.

$$F_D = \frac{18\mu}{\rho_p d_p^2}\frac{C_D R_e}{24} \quad \text{.....(6)}$$

Here, u denotes the fluid phase velocity, u_p the particle velocity, μ the molecular viscosity of the fluid, ρ the fluid density (7 800 kg m^{-3}), ρ_p the density of the particle (5 000 kg m^{-3}), and d_p the particle diameter. R_e denotes the relative Reynolds number, which is defined as

$$R_e = \frac{\rho d_p |u_p - u|}{\mu} \quad \text{.....(7)}$$

To simulate the chaotic effect of the turbulent eddies on the particle paths, a discrete random walk model is applied during inclusion trajectory calculations in which a random velocity vector, u'_p, is added to the calculated time-averaged vector, $\bar{u}_p$ to obtain the inclusion velocity u_p at each time step as it travels through the fluid. Each random component of the inclusion velocity is proportional to the local turbulent kinetic energy level, k according to the following equation.[4)]

$$u_p' = \zeta_i \sqrt{\overline{u_i'^2}} = \zeta_i \sqrt{\frac{2k}{3}} \quad \text{.....(8)}$$

Where ζ_i is a random number, normally distributed between -1 and 1 that changes at each time step. Inclusions are injected computationally at many different locations distributed homogeneously over the inlet plane. Each trajectory is calculated through the constant steel flow field until the inclusion either is trapped on the top surface or exits the tundish outlet.

3.2. Method of Calculation of Percentage Inclusion Removal

Statistics were gathered to quantify the fates of 1 080 inclusion trajectories for each particle size. The percentage inclusion removal[18)] from near outlet has been calculated as the percentage of total number of inclusion particles not being able to come out through the near outlet (N.O.) for a particular case. The similar methodology has been adopted to calculate the percentage inclusion removal from middle outlet (M.O.), far outlet (F.O.) and overall (sum of all the three outlets). **Table 3** shows the value of number of inclusion particles and percentage removal from all the three outlets as well as overall removal for different cases when the inclusion particle size is 30 μm.

3.3. Assumptions and Boundary Conditions

Flow is assumed to be steady and incompressible. Air and gas entrainment by incoming metal stream is neglected. The surface of tundish is considered to be perfectly flat and slag depth was considered to be insignificant. The generation of inclusions in the tundish due to any erosion of refractory or by any chemical reactions like deoxidation, *etc.*, was ignored. The 3-D domain of this tundish is divided into about 54 000 cells, with a fine mesh in the zone of the incoming and outgoing liquid jet in order to get high resolution in these complex zones and also to visualize in details the effects of velocity and turbulence gradients.

All velocities are set to zero at the wall (no slip condition). The wall functions are employed to compute the turbulence quantities in the vicinity of walls. The velocity

© 2008 ISIJ

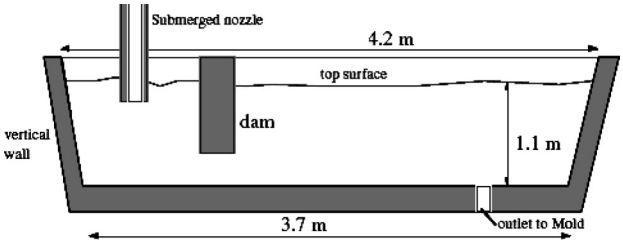


Fig. 2. Geometry of the single strand tundish for validation study.

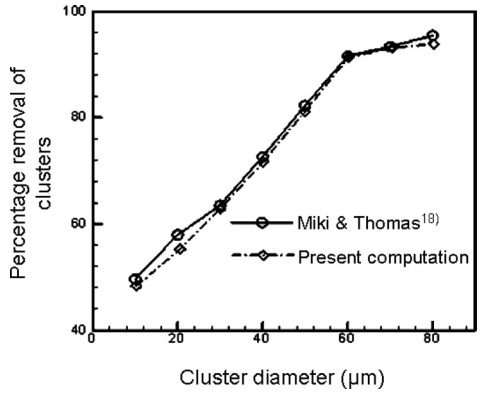


Fig. 3. Validation of present computational model with the work reported by Miki and Thomas.[18)]

components normal to planes of symmetry are set equal to zero. The upper top surface is assumed to be a free surface. At the inlet, the velocity is 1.4 m/s. Turbulence intensity at inlet is specified as 2%.

For inclusion trajectory removal cases, inclusions touching the sidewall are assumed to be reflected while those reaching the top surface are assumed to be trapped. Inclusions reaching the outlet are assumed to escape through it.

4. Results and Discussions

4.1. Validation of the Computational Model

Before proceeding with the computation on multi-strand tundish, the code has been validated against the literature reported work[18)] on a single strand tundish. The single strand tundish results on inclusion separation have been considered for validation because of unavailabity of reported literature on multi-strand tundish. **Figure 2** shows the tundish used for validation study[18)] and **Fig. 3** shows the comparative observation of the fraction of inclusion particles removed between present computational model and the reported work by Miki and Thomas.[18)] It can be seen that there is a reasonable match between the reported findings and the observed values by the present model.

4.2. Effect of Dam Height

Figures 4(a)–4(c) shows the variation of the percentage removal of inclusions from each outlet with varying dam heights at dam positions a, b and c, respectively. It can be seen that as the height of the dams is increased, the overall percentage removal of the inclusions increases. This is true for the dams at all the three positions. While the near outlet (N.O.) and middle outlet (M.O.) shows continuous increase in the inclusion removal at all the three dam positions, a decrease in the inclusion removal is observed from the far outlet (F.O.). The decrease in inclusion removal rate is more at position a, than at position b or c. It means that although the lower height dams (height 1) failed to improve the inclusions coming out of far outlet, increase in the dam height provides better results.

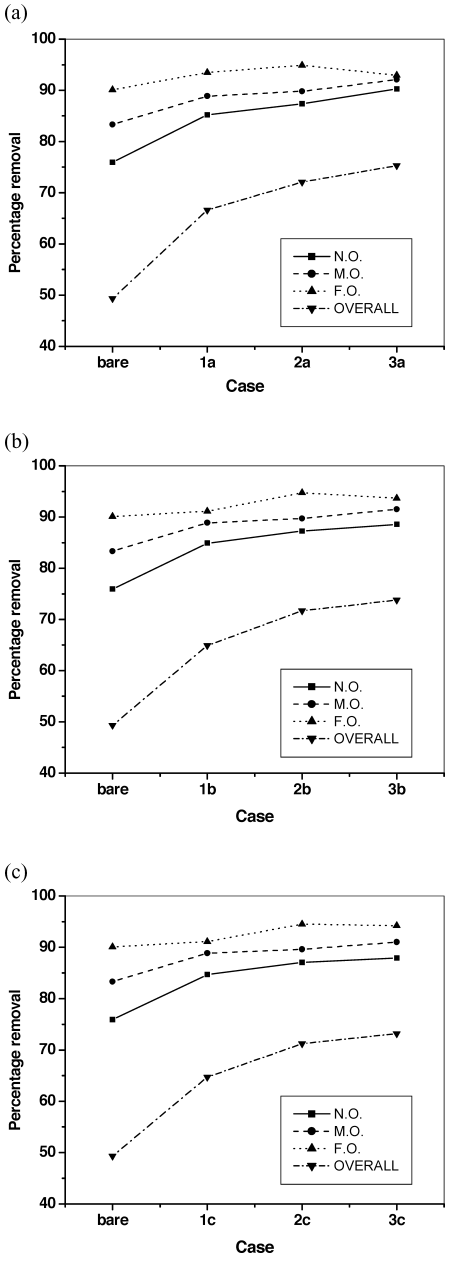


Fig. 4. Variation of percentage inclusion removal from each outlet and overall removal with increase in dam height at dam position-c (particle size=30 μm).

Further, it can be seen that at a particular position and for a particular height of dams (say case 1a), the percentage removal of inclusions differ for each of the three outlets, *i.e.*, the number of inclusions coming through the near outlet is the highest (lowest value of inclusion removal) and through the far outlet, it is the lowest. The billets coming out from the mold connected to these outlets are supposed to have uniform distribution of inclusions. This being the important objective of the steelmaker, a case which has minimum variation of inclusion distribution (inclusions coming out through the outlets) will be more ideal. It is clear that of the

© 2008 ISIJ

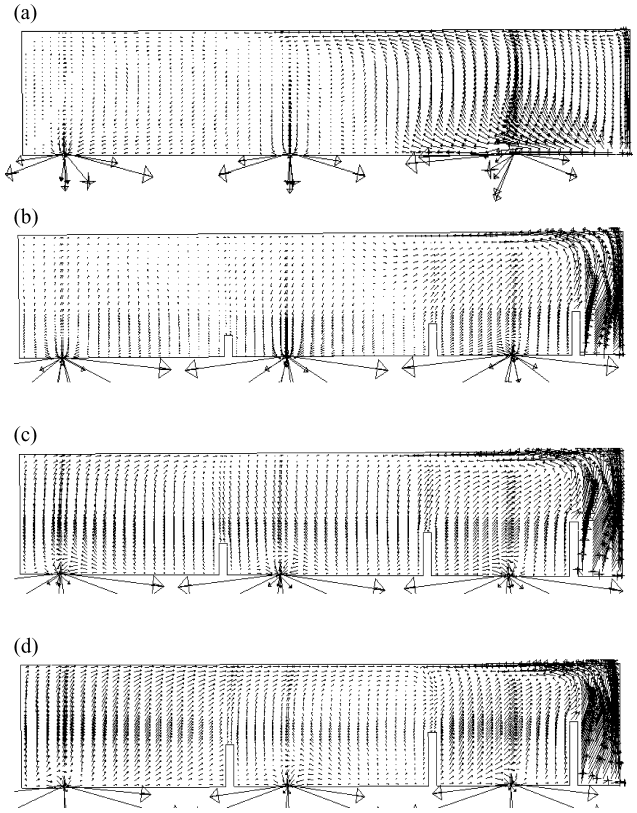


Fig. 5. Velocity field at a vertical plane passing through all the outlets for (a) bare tundish, (b) case 1a, (c) case 2a, (d) case 3a.

three heights used (height 1, 2 and 3) at different positions, case 3a (Fig. 4(a) shows the lowest band (difference in the inclusion removal rate from the three outlets). Therefore it can be inferred that dams of height 3 at position-a is the best for inclusion removal in a six strand tundish.

The reason for this increase in the inclusion removal can be understood with the help of velocity vectors drawn at a vertical plane passing through all the outlets for the bare tundish (**Fig. 5**(a)) and for the tundish with dams of varying height at position a (Figs. 5(b)–5(d)). In case of the bare tundish, the velocity field clearly suggests the presence of a recirculatory zone near the near outlet (NO) because of which inclusions are trapped in that zone and more number of inclusion particles come through the near outlet, indicating the minimum inclusion removal from the near outlet. As the dams are placed before the outlets, there can be seen a discernible change in the pattern of the velocity field. The short circuiting zone near the near outlet (NO) is no longer seen when the dams of height 1 are placed at position a (Fig. 5(a)). The inclusions get the tendency to flow towards the top surface because of the placement of the dams. The tendency of the particles to flow through the outlet is obstructed due to the presence of the dams before the outlets. Hence, the inclusion removal increases. As the height of the dams increases to 2 and 3 (at position a) (Figs. 4(c) and 4(d)), a more prominent top surface directed flow can be seen. Because of this, the inclusion removal increases with the increase in the height of the dams. Figure 5(d) (case 3a) suggests larger velocity near the far outlet as compared to Fig. 5(c) (case 2a) indicating the chance of inclusions exiting through the far outlet to be higher and so the inclusion

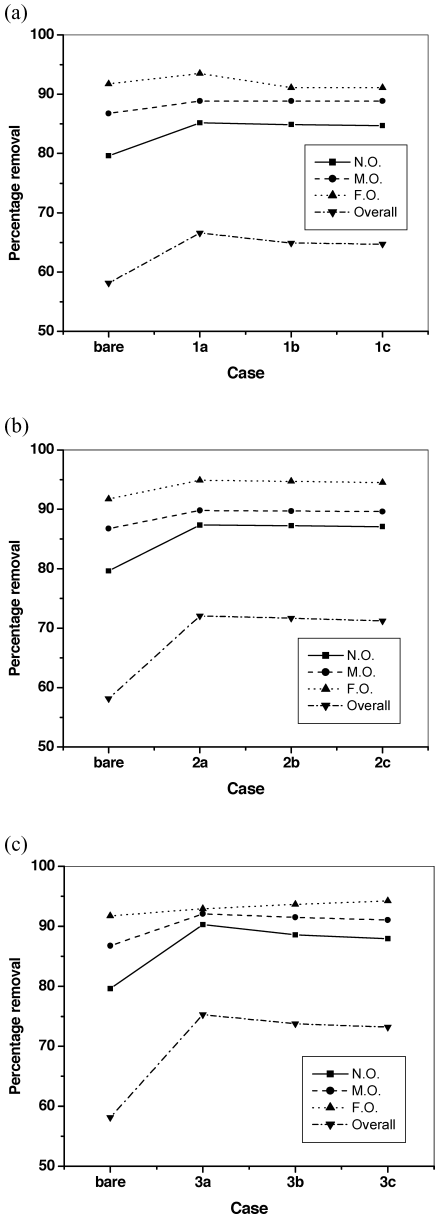


Fig. 6. Variation of percentage inclusion removal from each outlet and overall removal with change in positions of the dam (particle size=30 μm).

removal from the far outlet becomes less as the dam height is increased from height 2 to height 3 at position a. A more uniform velocity field suggests the minimum band (difference of inclusions coming through all the outlets).

4.3. Effect of Dam Positions

Figures 6(a)–6(c) shows the variation of inclusion removal with the change in the dam positions with dam heights at positions a, b and c, respectively. It can be seen from Fig. 6(a) that as the dams are moved towards the outlet (far from the inlet, case 1a to case 1b), the inclusion removal tendency decreases. This trend has been observed for all the dam heights Figs. 6(b) and 6(c). This can be better explained by referring to the velocity vectors in **Figs. 7**(a) and 7(b) (for case 1b and 1c, respectively). Comparing Fig. 5(a) with Fig. 7(a) (case 1a with case 1b), in the later case a recirculation zone is seen near the far outlet which traps the inclusions and makes it flow out through the far outlet. Due to this reason, the inclusion removal from the far outlet is

© 2008 ISIJ

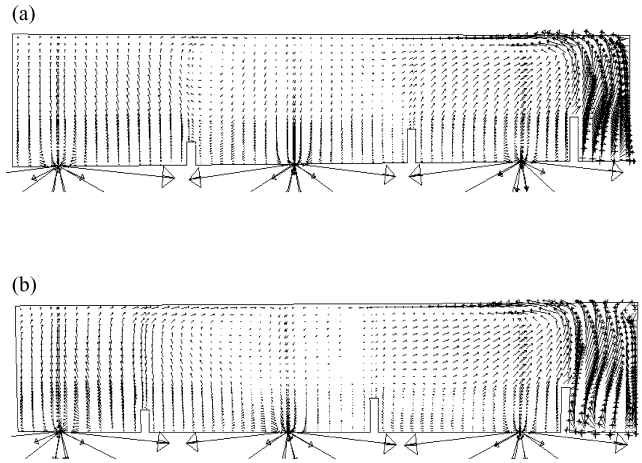


Fig. 7. Velocity field at a vertical plane passing through all the outlets for (a) case 1b and (b) case 1c.

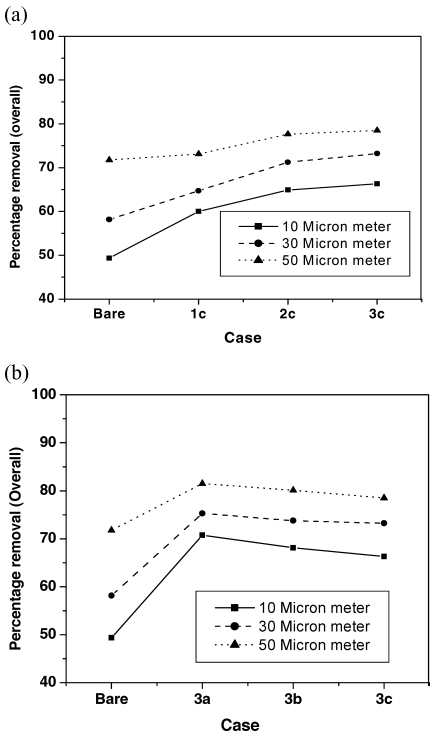


Fig. 8. Variation of percentage inclusion removal (overall) with change in particle size.

seen to decrease as the position is changed from a to b at height 1. There is not much change in the velocity pattern of case 1b and 1c which is indicated by the equal inclusion removal tendency by the two cases. It can also be seen clearly here that case 3a gives the minimum band for the inclusion removal by the three outlets and so this case, as found earlier, can be regarded as the case with best inclusion removal ability.

4.4. Effect of Inclusion Size

Figures 8(a) and 8(b) shows the variation of overall inclusion removal with change in particle sizes. While Fig. 8(a) shows the variation with dam height at position c, Fig. 8(b) shows the variation of percentage inclusion removal with different dam positions for dam height 3. Three different particle diameters were used in the study. It was seen that with an increase in particle size, there is an increase in the inclusion removal tendency. The trend of curves was seen to be same as found earlier (Figs. 4(c) and 6(c)).

5. Conclusions

Numerical investigation of inclusion removal process in a six-strand billet caster tundish has been carried out for bare tundish as well as for tundish with dams of different heights and at different locations. Dimensionless heights (ratio of dam height to tundish height) and dimensionless distance (ration of distance of dam from inlet to tundish half length) have been used as the two geometrical parameters which have been varied to see its effect on the inclusion removal rate in a six-strand billet caster tundish. It was observed that the inclusion removal tendency increases with the use of dams as compared to the bare tundish. It was also found that at a particular position of the dams, inclusion removal tendency increases with increase in dam heights. However, for a particular combination of dam heights, as the dams were moved closer to the outlets (with increase of dimensionless distance) the inclusion removal tendency was seen to decrease. When the dams are moved close to the outlets, the presence of recirculation zone near the far outlet region is expected to increase the tendency of inclusions passing through the far outlet, thereby reducing the inclusion removal. The maximum difference of number of inclusion particles from all the three outlets (band) was observed to be least for the case 3a, *i.e.*, when the dimensionless heights of the near, middle and far dams are 0.52, 0.44 and 0.35 and dimensionless distances of these dams from the inlet are 0.09, .32 and 0.66 respectively.

Nomenclature

F: Body forces
G: Gravitational acceleration
k: Turbulent kinetic energy
p: Pressure
t: Time
u_i: Velocity
x: Coordinate for measure of distance
ρ: Density of the fluid
μ: Co-efficient of viscosity
ν: Kinematic viscosity
$\overline{u_i u_j}$: Average turbulent stress
ε: Rate of dissipation of turbulent kinetic energy
σ_c: Turbulent Schmidt number
ϕ: Either k or ε

Suffix
i, j, k: Three Cartesian coordinate directions x, y and z
eff: Effective
p: Particle
t: Turbulent

REFERENCES

1) H. Tanaka, R. Nishihara, I. Kitagawa and R. Tsujino: *ISIJ Int.*, **33** (1993), 1238.
2) O. Ilegbusi and J. Szekely: The Physical and Mathematical Modeling of Tundish Operations, Springer-Verlag, New-York, (1989), 56
3) H. Tacke and J. C. Ludwig: *Steel Res.*, **58** (1987), 262.
4) H. B. Kaufmann, A. Niedermayr, H. Sattler and A. Preuer: *Steel Res.*, **64** (1993), 203.

© 2008 ISIJ

5) D. Mazumdar and R. I. L. Guthrie: *ISIJ Int.*, **39** (1999), 524.
6) Y. Sahai and R. Ahuja: *Ironmaking Steelmaking*, **13** (1986), 241.
7) J. Tsukobura, I. D. Sommerville and A. McLean: 24th Annual Conf. of Metallurgists, CIM, Canada, (1985), 124.
8) Youduo He and Y. Sahai: *Acta Metall. Sin.*, **2** (1988), 93.
9) J. Szekely, O. J. Illegbusi and N. El-Kaddah: *Phys. Chem. Hydrod.*, **9** (1987), 453.
10) P. K. Jha, S. K. Dash and S. Kumar: *ISIJ Int.*, **41** (2001), 1437.
11) S. C. Koria and S. Singh: *Ironmaking Steelmaking*, **20** (1993), 221.
12) K. Tozawa, Y. Kato and T. Nakanishi: *CAMP-ISIJ*, **10** (1997), 105.
13) A. K. Sinha and Y. Sahai: *ISIJ Int.*, **33** (1993), 556.
14) O. J. Ilegbusi and J. Szekely: *ISIJ Int.*, **29** (1989), 1031.
15) S. Joo and R. I. L. Guthrie: *Metall. Trans.*, **24B** (1993), 755.
16) E. Martinez, M. Maeda, L. J. Heaslip, G. Rodriguez and A. McLean: *Trans. Iron Steel Inst. Jpn.*, **26** (1986), 724.
17) S. Joo and R. I. L. Guthrie: *Can. Metall. Q.*, **30** (1991), 261.
18) Y. Miki and B. G. Thomas: *Metall. Trans.*, **30B** (1999), 639.
19) L. Zhang and B. G. Thomas: XXIV Steel Making National Symposium, Morelia, Mich, Mexico, (2003), 184.
20) FLUENT users guide Vol. 1–4, Fluent Inc., Lebanon, NH, (1995).
21) B. E. Launder and D. B. Spalding: Mathematical Models of Turbulence, Academic Press, London, (1972), 90.

© 2008 ISIJ